J|A|C|S
ARTICLES
Published on Web 07/25/2006

Synthesis and Reactivity of the Imido Analogues of the Uranyl Ion

Trevor W. Hayton,[†] James M. Boncella,*[,†] Brian L. Scott,[†] Enrique R. Batista,[‡] and P. Jeffrey Hay[‡]

Contribution from the Chemistry Division, Los Alamos National Laboratory, MS J514, and Theoretical Division, Los Alamos National Laboratory, MS B268, Los Alamos, New Mexico 87545

Received May 4, 2006; E-mail: boncella@lanl.gov

Abstract: Addition of 1.5 equiv of I_2 to a THF solution of $UI_3(THF)_4$, containing either 6 equiv of $^tBuNH_2$ or 2 equiv of RNH_2 (R = Ph, 3,5-$(CF_3)_2C_6H_3$, 2,6-$(^iPr)_2C_6H_3$) and 4 equiv of NEt_3, generates orange solutions containing $U(N^tBu)_2I_2(THF)_2$ (**1**) or $U(NAr)_2I_2(THF)_3$ (Ar = Ph, **2**; 3,5-$(CF_3)_2C_6H_3$, **3**; 2,6-$(^iPr)_2C_6H_3$, **4**), respectively, all of which can be isolated in good yields. Alternatively, **1** can be prepared by reaction of uranium metal with 3 equiv of I_2 and 6 equiv of $^tBuNH_2$, also in good yield. Complexes **1**−**4** have been characterized by X-ray crystallography, and each of these complexes exhibits linear N−U−N linkages and short U−N bonds. Using density functional theory simulations of complexes **1** and **2**, two triple bonds between the metal center and the nitrogen ligands were identified. Complexes **1** and **2** readily react with neutral Lewis bases such as pyridine or Ph_3PO to form $U(NR)_2I_2(L)_2$ (R = ^{t}Bu, L = py, **5**; Ph_3PO, **7**; R = Ph, L = py, **6**; Ph_3PO, **8**), and with PMe_3 to form $U(NR)_2I_2(THF)(PMe_3)_2$ (R = ^{t}Bu, **9**; Ph, **10**). The solid-state molecular structures of **5**, **7**, and **9** have been determined by X-ray crystallography, and these complexes, like their parent compounds, exhibit linear N−U−N angles and short U−N bonds. Complexes **1** and **2** also react with AgOTf in CH_2Cl_2, forming $U(NR)_2(OTf)_2(THF)_3$ (R = ^{t}Bu, **11**; Ph, **12**) after recrystallization from THF. Crystals of **12** grown from CH_2Cl_2 were found to contain a dimer, $[U(NPh)_2(OTf)_2(THF)_2]_2$, a complex possessing bridging triflate groups.

Introduction

Since the discovery of the first uranium imido complex over 20 years ago by Andersen and co-workers,[1] the chemistry of this functional group has been the focus of many actinide chemists. The research inspired by this initial discovery has led to the synthesis of a variety of uranium imido complexes in which the metal varies in oxidation state from +4 to +6. For instance, Andersen was also able to synthesize $U(NSiMe_3)(N\{SiMe_3\}_2)_3$,[2] while Burns and co-workers have isolated $Cp^*_2U(NR)_2$ (R = Ph, adamantyl),[3−5] $Cp^*_2U(O)(N\text{-}2,6\text{-}(^iPr)_2C_6H_3)$,[6] and $Cp^*_2U(N\text{-}2,4,6\text{-}(^tBu)_3C_6H_2)$.[4] In addition, several heteroatom-substituted imido complexes are known for uranium, such as $Cp_3U(NPPh_3)$ and $Cp^*_2U(NSPh_2)_2$.[7,8] Bridging imido ligands are also known for uranium, as in the case of the U(IV) compounds $[(Cp')_2U(\mu\text{-}NR)]_2$ (Cp′ = MeCp, R = Ph; Cp′ = 1,3-$(SiMe_3)_2C_5H_3$, R = H).[9,10] The presence of a uranium−nitrogen multiple bond in these complexes suggests that there may be a significant covalent interaction between the metal and the nitrogen atom. Such covalency challenges the conventional wisdom that the bonding in actinide compounds is primarily ionic in nature and does not involve a significant contribution from the valence 5f and 6d orbitals on the metal center.

The obvious similarity between the oxo ligand and the imido group has made the synthesis of an imido analogue of the uranyl ion highly desirable. Uranyl (UO_2^{2+}) is the most prevalent functional unit in the chemistry of U(VI) and has been known for more than 150 years.[11] With the advent of nuclear energy and the use of uranium oxide as a reactor fuel, the chemistry of the uranyl ion has played an essential role in the processing of uranium ore, nuclear fuel, and waste.[12] The linear arrangement of the oxo ligands, extremely short U−O bonds, and high thermal and chemical stability reflect some of the unique properties of this moiety.[13]

Recently, we discovered a simple, general, high-yield procedure for the synthesis of a family of bis(imido) uranium(VI) diiodide complexes, the imido analogues of the uranyl ion.[14]

[†] Chemistry Division.
[‡] Theoretical Division.

(1) Brennan, J. G.; Andersen, R. A. *J. Am. Chem. Soc.* **1985**, *107*, 514−516.
(2) Zalkin, A.; Brennan, J. G.; Andersen, R. A. *Acta Crystallogr., Sect. C* **1988**, *44*, 1553−1554.
(3) Arney, D. S. J.; Burns, C. J.; Smith, D. C. *J. Am. Chem. Soc.* **1992**, *114*, 10068−10069.
(4) Arney, D. S. J.; Burns, C. J. *J. Am. Chem. Soc.* **1995**, *117*, 9448−9460.
(5) Warner, B. P.; Scott, B. L.; Burns, C. J. *Angew. Chem., Int. Ed.* **1998**, *37*, 959−960.
(6) Arney, D. S. J.; Burns, C. J. *J. Am. Chem. Soc.* **1993**, *115*, 9840−9841.
(7) Cramer, R. E.; Edelmann, F.; Mori, A. L.; Roth, S.; Gilje, J. W.; Tatsumi, K.; Nakamura, A. *Organometallics* **1988**, *7*, 841−849.
(8) Ariyaratne, K. A. N. S.; Cramer, R. E.; Gilje, J. W. *Organometallics* **2002**, *21*, 5799−5802.
(9) Brennan, J. G.; Andersen, R. A.; Zalkin, A. *J. Am. Chem. Soc.* **1988**, *110*, 4554−4558.
(10) Zi, G.; Blosch, L. L.; Jia, L.; Andersen, R. A. *Organometallics* **2005**, *24*, 4602−4612.
(11) Comyns, A. E. *Chem. Rev.* **1960**, *60*, 115−146.
(12) Katz, J. J.; Seaborg, G. T.; Morss, L. R. *The Chemistry of the Actinide Elements*, 2nd ed.; Chapman and Hall: New York, 1986; Vol. 1.
(13) Denning, R. G. *Struct. Bonding* **1992**, *79*, 215−276.

The ability to obtain these complexes presents a unique opportunity to expand the chemistry of U(VI) and to study the trans disposition of two imido ligands, an arrangement that is exceedingly rare. In addition, the ease of synthesis of the bis(imido) complexes makes them attractive as starting materials for the isolation of a variety of new derivatives.

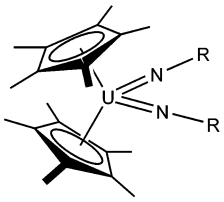

A

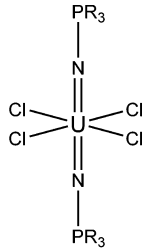

B

Until our recent report, the closest imido analogues to the uranyl ion were the bent, bis(imido) complexes synthesized by Burns and co-workers (**A**), and the zwitterionic phosphoriminato complex synthesized by Denning et al. (**B**)[15,16] and studied using electronic structure calculations by Kaltsoyannis.[17] In the case of the bent bis(imido) complexes, the bulky pentamethylcyclopentadienyl ancillary ligands provide a significant degree of kinetic stabilization that limits the reactivity of the U=N bond. Furthermore, the acute N=U=N angle leads to a different bonding interaction between the metal center and the N−R groups relative to a complex with a linear N=U=N arrangement. The phosphoriminato complexes, while preserving the linear N=U=N structure of uranyl, have a significant contribution from a resonance form that is best described as having a U−N single bond. Thus, neither **A** nor **B** duplicates the combination of structural and electronic properties that a true imido analogue of the uranyl ion would have.

In this report, we describe the synthesis of four complexes with the general formula $U(NR)_2I_2(THF)_x$ ($x = 2$, 3), and the reactivity of these complexes with a variety of Lewis bases, and AgOTf. The nature of the chemical bonding between the uranium center and the nitrogen ligands was studied using ab initio density functional calculations and is described in detail.

Results and Discussion

Synthesis of Uranium Bis(imido) Complexes. The reaction of uranium turnings with I_2 (3 equiv) and *tert*-butylamine (6 equiv) in THF quickly results in metal dissolution and the formation of an orange solution (eq 1). Recrystallization of the resulting orange material from a toluene/hexanes solution provides $U(N^tBu)_2I_2(THF)_2$ (**1**) in high yield.

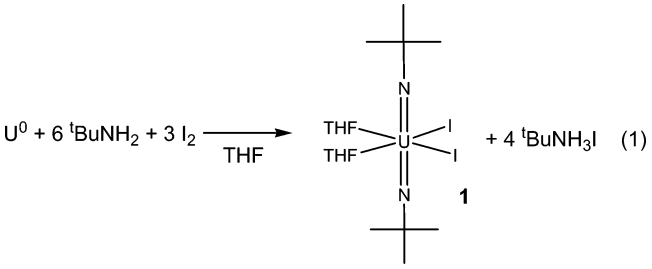

Replacing *tert*-butylamine with aniline in eq 1 does not provide any tractable products. However, by using $UI_3(THF)_4$ as the uranium source, and by adding a strong base such as triethylamine, a bis(imido) complex could be made in high yield. Thus, addition of 1.5 equiv of I_2 to a THF solution of $UI_3(THF)_4$, $ArNH_2$ (2 equiv), and NEt_3 (4 equiv) generates orange-brown solutions containing $U(NAr)_2I_2(THF)_3$ (Ar = Ph, **2**; 3,5-$(CF_3)_2C_6H_3$, **3**; 2,6-$(^iPr)_2C_6H_3$, **4**) (eq 2). The methodology outlined in eq 2 appears to be readily adaptable to the synthesis of a large number of imido complexes, simply by changing the primary amine. Indeed, complex **1** can also be made from $UI_3(THF)_4$ in high yield.

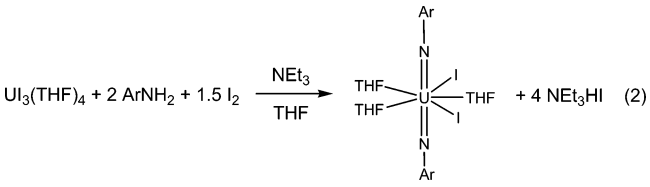

Ar = Ph, **2**; 3,5-$(CF_3)_2C_6H_3$, **3**; 2,6-$(^iPr)_2C_6H_3$, **4**

Complex **1** is an orange, moisture-sensitive crystalline solid, which is soluble in THF and toluene. The ^1H NMR spectrum of **1** displays resonances for both THF ligands and *tert*-butyl groups, in a 1:1 ratio. Complexes **2** and **3** are red-brown crystalline solids with solubility properties similar to those of **1**. The ^1H NMR spectrum of **2** exhibits resonances for three equivalent THF ligands and two equivalent phenyl moieties, while complex **3** also exhibits resonances in its ^1H NMR spectrum consistent with the presence of three equivalent THF ligands and two imido groups. In addition, its ^{19}F NMR spectrum consists of a single peak at −64.0 ppm. Broad resonances for three equivalent THF ligands, as well as resonances for four equivalent isopropyl groups, are observed in the ^1H NMR spectrum of **4** at room temperature.

The chemically equivalent THF ligands of **2**, **3**, and **4** contrast with their solid-state molecular structures (vide infra), suggesting exchange of the two types of THF ligands. Rapid exchange between free and coordinated THF was confirmed when THF was added to NMR samples of **2**. In the presence of excess THF, the THF resonances of **2** are shifted from 4.38 and 1.41 ppm to the values anticipated for free THF (3.57 and 1.40 ppm), suggesting exchange of coordinated and uncoordinated THF molecules. Given the facile exchange of THF, it is likely that two types of THF ligands can exchange similarly, via a dissociative mechanism.

The IR spectra of complexes **1** and **2** show strong vibrations at 1170 and 1270 cm^{-1}, respectively, which are in the region expected for a trans imido complex.[18] The UV/vis spectra of **1** and **2** each display two intense, broad maxima. For **1**, the absorption bands occur at 291 nm ($\epsilon = 3500$ L mol^{-1} cm^{-1}) and 353 nm ($\epsilon = 2200$ L mol^{-1} cm^{-1}), whereas for **2** they are observed at 291 nm ($\epsilon = 7900$ L mol^{-1} cm^{-1}) and 352 nm ($\epsilon = 1900$ L mol^{-1} cm^{-1}). The vibronic coupling fine-structure often seen in uranyl UV/vis spectra is not observed for **1** and **2**. The lack of fine structure is understandable given that the U−N stretching modes are coupled with other vibrational modes of the substituents of the imido ligands.

(14) Hayton, T. W.; Boncella, J. M.; Palmer, P. D.; Scott, B. L.; Batista, E. R.; Hay, P. J. *Science* **2005**, *310*, 1941−1943.
(15) Brown, D. R.; Denning, R. G. *Inorg. Chem.* **1996**, *35*, 6158−6163.
(16) Brown, D. R.; Denning, R. G.; Jones, R. H. *Chem. Commun.* **1994**, 2601−2602.
(17) Kaltsoyannis, N. *Inorg. Chem.* **2000**, *39*, 6009−6017.
(18) Li, Z.-Y.; Huang, J.-S.; Chan, M. C.-W.; Cheung, K.-K.; Che, C.-M. *Inorg. Chem.* **1997**, *36*, 3064−3071.

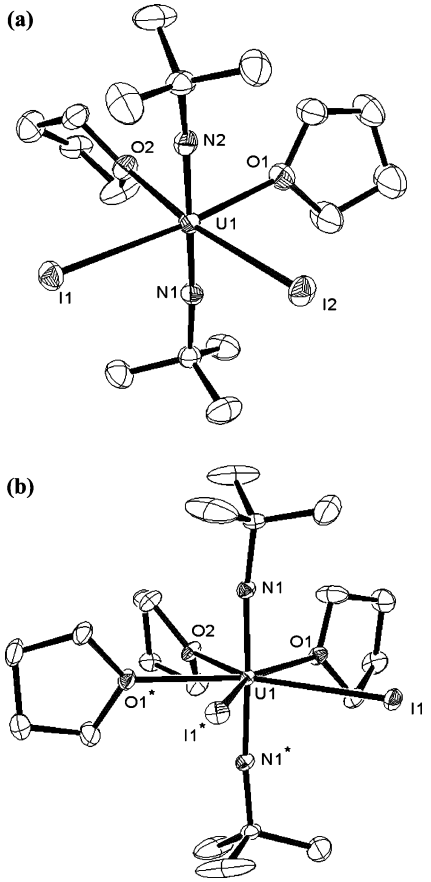

Figure 1. Solid-state molecular structures of $U(N^tBu)_2I_2(THF)_2$ (**1**) and $U(N^tBu)_2I_2(THF)_3$ (**1a**) with 50% probability ellipsoids shown. Selected bond lengths (Å) and angles (deg) for **1**: U1−N1 = 1.848(4), U1−N2 = 1.840(4), U1−O1 = 2.429(4), U1−O2 = 2.401(3), U1−I1 = 3.0571(4), U1−I2 = 3.0502(4), N1−U1−N2 = 175.4(2), U1−N1−C1 = 167.7(3), U1−N2−C5 = 168.9(4). Selected bond lengths (Å) and angles (deg) for **1a**: U1−N1 = 1.855(2), U1−O1 = 2.490(2), U1−O2 = 2.534(2), U1−I1 = 3.1371(2), N1−U1−N1* = 175.6(1), U1−N1−C7 = 166.3(2).

The solid-state molecular structures for **1**, **2**, **3**, and **4** have all been determined. Large X-ray quality crystals of **1** were grown by layering hexanes onto a THF solution of **1** at room temperature, and the structure of complex **1** is shown in Figure 1a. In addition, we have also isolated a second species from cold THF solutions of **1**, $U(N^tBu)_2I_2(THF)_3$ (**1a**), as shown in Figure 1b. Complex **1** exhibits an octahedral geometry, while **1a** exhibits pentagonal bipyramidal coordination. Both geometries are common for the uranyl ion. The two linear imido ligands in **1** exhibit a trans geometry (N1−U1−N2 = 175.4(2)°) and short U−N bonds (U1−N1 = 1.848(4) Å, U1−N2 = 1.840(4) Å). The bis(imido) unit in **1a** is nearly identical (U1−N1 = 1.855(2) Å, N1−U1−N1* = 175.6(1)°). The U−I bond lengths in **1** and **1a** are U1−I1 = 3.0571(4) Å and U1−I2 = 3.0502(4) Å, and U1−I1 = 3.1371(2) Å, respectively.

Like **1a**, complex **2** also exhibits a pentagonal bipyramidal geometry; however, in this instance the third THF ligand coordinates between the two iodide ligands (Figure 2). Complex **2** also exhibits trans, linear imido ligands and short U−N bonds (U1−N1 = 1.866(2) Å, U1−N2 = 1.859(2) Å, N1−U1−N2 = 177.42(9)°). The other metrical parameters of **2** are similar to those of **1** and **1a**.

Complex **3** was found to crystallize in the orthorhombic space group $Pbc2_1$ with two independent molecules in the asymmetric unit, and the solid-state molecular structure of one molecule is shown in Figure 3. Its bis(imido) framework is similar to that of **2**, with nearly identical U−N bond lengths (U2−N3 = 1.86(1) Å, U2−N4 = 1.89(1) Å), and a linear N−U−N angle (N3−U2−N4 = 176.8(4)°). Furthermore, the U−O and U−I bond lengths of **3** are comparable to those observed in **2**. Thus, it appears that the electron-withdrawing CF_3 groups in **3** do not have an appreciable effect on the bonding in the bis(imido) framework.

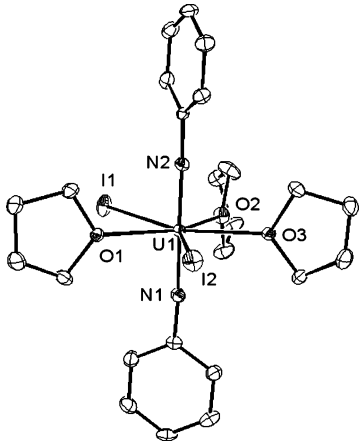

Figure 2. Solid-state molecular structure of $U(NPh)_2I_2(THF)_3$ (**2**). Selected bond lengths (Å) and angles (deg): U1−N1 = 1.866(2), U1−N2 = 1.859(2), U1−O1 = 2.418(2), U1−O2 = 2.452(2), U1−O3 = 2.4632(2), U1−I1 = 3.1378(3), U1−I2 = 3.1207(2), N1−U1−N2 = 177.42(9), U1−N1−C7 = 176.2(2), U1−N2−C1 = 177.7(2).

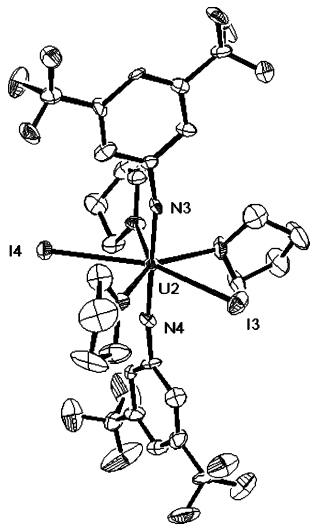

Figure 3. Solid-state molecular structure of $U(N\{C_6H_3\text{-}3,5\text{-}(CF_3)_2\})_2I_2(THF)_3$ (**3**). Selected bond lengths (Å) and angles (deg): U2−N3 = 1.86(1), U2−N4 = 1.89(1), U2−O5 = 2.42(1), U2−O4 = 2.43(1), U2−O6 = 2.45(1), U2−I3 = 3.126(1), U2−I4 = 3.115(1), N3−U2−N4 = 176.8(4), C37−N4−U2 = 169.1(9), C29−N3−U2 = 168.1(9).

Complex **4** crystallizes in the monoclinic space group $P2_1/c$ as the THF solvate **4**·THF. Its solid-state molecular structure is shown in Figure 4. The bis(imido) framework in **4** is nearly identical to that seen in **2** and **3**. It exhibits short U−N bonds (U1−N1 = 1.886(3) Å, U1−N2 = 1.888(3) Å) and a linear N−U−N angle (N1−U1−N2 = 169.3(1)°). Unlike those complexes though, the coordination sphere of complex **4** is notably distorted from an ideal pentagonal bipyramidal geometry. Looking down the O1−U1 vector (Figure 4b) shows a significant displacement of two THF ligands out of the I1−

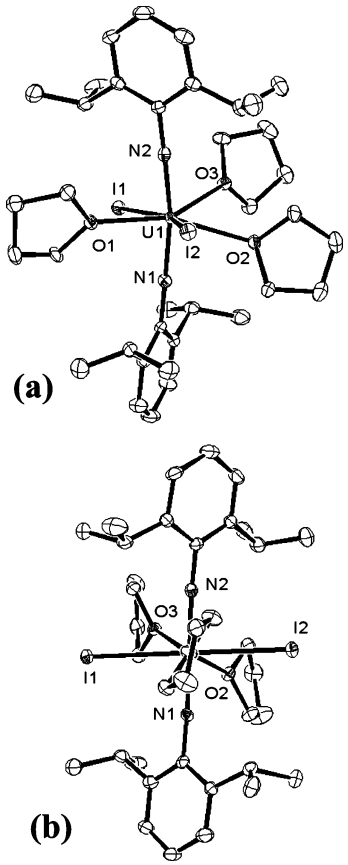

Figure 4. Solid-state molecular structure of $U(N\{C_6H_3\text{-}2,6\text{-}(^iPr)_2\})_2I_2(THF)_3\cdot THF$ (**4**·THF). Selected bond lengths (Å) and angles (deg): U1−N1 = 1.886(3), U1−N2 = 1.888(3), U1−O1 = 2.431(3), U1−O2 = 2.541(3), U1−O3 = 2.530(3), N1−U1−N2 = 169.3(1), N1−U1−O3 = 110.2(1), N2−U1−O2 = 109.6(1), C1−N1−U1 = 176.9(3), C13−N2−U1 = 174.5(3).

U1−I2 plane. This is also exemplified by the N−U−O angles, which deviate from the expected 90° (N1−U1−O3 = 110.2(1)°, N2−U1−O2 = 109.6(1)°). This deviation is no doubt caused by the bulky isopropyl groups on the phenyl ring.

The U−N bonds in **1**, **2**, **3**, and **4** are significantly shorter than the U−N bonds reported for $[PPh_4][UOCl_4(NSPh_2)]$ and $[PPh_4][UOCl_4(NPPh_3)]$ (1.920(3) and 1.912(3) Å, respectively).[19] They are also much shorter than those observed in other uranium imido species, for example, $Cp^*_2U(NPh)_2$ (U−N = 1.952(7) Å),[3] $Cp^*_2U(NAd)_2$ (av. U−N = 1.95 Å),[5] and $U(NSiMe_3)(N\{SiMe_3\}_2)_3$ (U−N = 1.910(6) Å),[2] but are comparable to the U−N bond in $U[N(SiMe_3)_2]_3(NSiMe_3)(F)$ (U−N = 1.85(2) Å).[20] A number of uranyl iodide complexes have also been structurally characterized,[21−24] and they exhibit U−I metrical parameters similar to those of complexes **1**−**4**. The U−O bond lengths in **1**, **2**, **3**, and **4** are comparable to the U−O distances in related uranyl THF complexes.[25−27]

Many bis(imido) complexes are known for the transition metals. For instance, several group 6 bis(imido) complexes of the type $M(NR)_2Cl_2L_2$ (where M is Mo or W, and L is a neutral Lewis base) are known.[28−30] In each of these derivatives, the imido functionalities are in a cis arrangement with respect to each other. The trans arrangement of the imido ligands is quite rare[18,31−33] and has only been observed when the substituents on the imido ligands and the co-ligands are quite bulky (as in $Os(N\text{-}2,6\text{-}(^iPr)_2C_6H_3)_2(PMe_2Ph)_2$),[31] or when the co-ligand is a porphyrin (as in $Os(N^tBu)_2$(tetrakis(4-clorophenyl)porphyrinato).[18,34,35] For comparison, in $Os(N\text{-}2,6\text{-}(^iPr)_2C_6H_3)_2(PMe_2Ph)_2$, the Os−N bond length is 1.790(6) Å.[33]

The oxidation of uranium metal with I_2 in organic solvents generally leads to either U(III)- or U(IV)-containing products.[36−38] The isolation or observation of a U(VI) species is unprecedented under those conditions. Interestingly, neither UI_6 nor UI_5 is known to exist, and UI_4 slowly disproportionates to UI_3 and I_2.[39] Thus, the formation of the U−N multiple bonds plays a significant role in providing a thermodynamic driving force over and above the oxidizing power of I_2 to facilitate this reaction. The strength of the U−N interactions in **1**−**4** is also consistent with the short U−N bond lengths that are observed in the solid state. In addition, the competency of $UI_3(THF)_4$ as a uranium source in the formation of $U(NR)_2I_2(THF)_x$ (x = 2, 3) suggests that other U(III), and possibly U(IV), coordination complexes could also be precursors to a bis(imido) species. Interestingly, under no circumstance do we observe a reaction between $UI_3(THF)_4$ and the primary amine, even in the presence of NEt_3. As such, it is likely that uranium must be oxidized to U(IV) before the amine can react with the metal complex. In this regard, the U(IV) tris(amide) complex $[U(NH^tBu)_3(NH_2^tBu)_3]^+$ has been isolated by Ephritikhine and co-workers,[40] and this species or a similar complex represents a possible intermediate in the formation of complex **1** from uranium metal. Finally, when eq 1 is performed with an excess of uranium metal the only product isolated is **1**, and unreacted metal remains in the reaction flask.

Analysis of the Chemical Bonding. The chemical bonding in uranium imido complexes was analyzed using density

(19) Williams, V. C.; Müller, M.; Leech, M. A.; Denning, R. G.; Green, M. L. H. *Inorg. Chem.* **2000**, *39*, 2538−2541.
(20) Burns, C. J.; Smith, W. H.; Huffman, J. C.; Sattelberger, A. P. *J. Am. Chem. Soc.* **1990**, *112*, 3237−3239.
(21) Crawford, M.-J.; Ellern, A.; Karaghiosoff, K.; Mayer, P.; Nöth, H.; Suter, M. *Inorg. Chem.* **2004**, *43*, 7120−7126.
(22) Crawford, M.-J.; Ellern, A.; Nöth, H.; Suter, M. *J. Am. Chem. Soc.* **2003**, *125*, 11778−11779.
(23) Berthet, J.-C.; Nierlich, M.; Ephritikhine, M. *Chem. Commun.* **2004**, 870−871.
(24) Crawford, M.-J.; Mayer, P. *Inorg. Chem.* **2005**, *44*, 5547−5549.
(25) Charpin, P.; Lance, M.; Nierlich, M.; Vigner, D. C. B. *Acta Crystallogr., Sect. C* **1987**, *43*, 1832−1833.
(26) Rebizant, J.; Van den Bossche, G.; Spirlet, M. R.; Goffart, J. *Acta Crystallogr., Sect. C* **1987**, *43*, 1298−1300.
(27) Wilkerson, M. P.; Burns, C. J.; Paine, R. T.; Scott, B. L. *Inorg. Chem.* **1999**, *38*, 4156−4158.
(28) del Rio, D.; Montilla, F.; Pastor, A.; Galindo, A.; Monge, A.; Gutiérrez-Puebla, E. *J. Chem. Soc., Dalton Trans.* **2000**, 2433−2437.
(29) Danopoulos, A. A.; Wilkinson, G.; Hussain-Bates, B.; Hursthouse, M. B. *J. Chem. Soc., Dalton Trans.* **1990**, 2753−2761.
(30) Ashcroft, B. R.; Bradley, D. C.; Clark, G. R.; Errington, J.; Nielson, A. J.; Rickard, C. E. F. **1987**, 170−171.
(31) Anhaus, J. T.; Kee, T. P.; Schofield, M. H.; Schrock, R. R. *J. Am. Chem. Soc.* **1990**, *112*, 1642−1643.
(32) Danopoulos, A. A.; Wilkinson, G.; Hussain-Bates, B.; Hursthouse, M. B. *Polyhedron* **1992**, *11*, 2961−2964.
(33) Schofield, M. H.; Kee, T. P.; Anhaus, J. T.; Schrock, R. R.; Johnson, K. H.; Davis, W. M. *Inorg. Chem.* **1991**, *30*, 3595−3604.
(34) Smieja, J. A.; Omberg, K. M.; Breneman, G. L. *Inorg. Chem.* **1994**, *33*, 614−616.
(35) Smieja, J. A.; Shirzad, K.; Roy, M.; Kittilstved, K.; Twamley, B. *Inorg. Chim. Acta* **2002**, *335*, 141−146.
(36) Avens, L. R.; Bott, S. G.; Clark, D. L.; Sattelberger, A. P.; Watkin, J. G.; Zwick, B. D. *Inorg. Chem.* **1994**, *33*, 2248−2256.
(37) Enriquez, A. E.; Scott, B. L.; Neu, M. P. *Inorg. Chem.* **2005**, *44*, 7403−7413.
(38) Evans, W. J.; Kozimor, S. A.; Ziller, J. W.; Fagin, A. A.; Bochkarev, M. N. *Inorg. Chem.* **2005**, *44*, 3993−4000.
(39) Cotton, F. A.; Wilkinson, G.; Murillo, C. A.; Bochmann, M. *Advanced Inorganic Chemistry*, 6th ed.; John Wiley & Sons: New York, 1999; pp 1146−1147.
(40) Wang, J. X.; Dash, A. K.; Kapon, M.; Berthet, J.-C.; Ephritikhine, M.; Eisen, M. S. *Chem.-Eur. J.* **2002**, *8*, 5384−5396.

Table 1. Mulliken Populations and Orbital Energies for the Six Molecular Orbitals Involved in the U−N Bonds of $U(NMe)_2I_2(THF)_2$[a]

		U						N_a	N_b
	ϵ [eV]	s	p	d	f	total	type	total	total
HOMO−6	−7.129	0.000	0.005	0.012	0.320	0.337	f_π	0.238	0.243
HOMO−7	−7.193	0.017	0.002	0.025	0.272	0.316	f_π	0.218	0.248
HOMO−8	−7.314	0.000	0.026	0.131	0.232	0.389	$f_\sigma + d_\pi$	0.254	0.203
HOMO−9	−7.528	0.000	0.000	0.240	0.002	0.242	d_π	0.254	0.263
HOMO−12	−8.665	0.000	0.079	0.080	0.243	0.402	f_σ	0.195	0.198
HOMO−21	−11.394	0.006	0.001	0.101	0.019	0.127	d_σ	0.193	0.197

[a] The populations are given in fractions of an electron. The type of uranium atomic orbital involved in each of the bonding molecular orbitals is identified in the "type" column.

functional calculations on complexes **1** and **2** with four and five equatorial ligands, respectively. In all cases, the B3LYP hybrid density functional was used.[41] For the sake of reducing the computational cost, in complex **1** we used a model system that replaced the ^{t}Bu groups in the ligands with methyl groups. The similarities in the bonding analysis between $U(NMe)_2I_2(THF)_2$ and **2** and the closeness in the predicted and experimental bond distances indicate that this simplification did not affect the U−N bonding.

To validate the computational methodology, the structures of $U(NMe)_2I_2(THF)_2$ and complex **2** were optimized and compared to the experimental ones. For $U(NMe)_2I_2(THF)_2$, the calculated U−N distances (1.844 Å) and U−I distances (3.058 Å) were found to be within 0.005 Å of the observed measurements of complex **1**. For complex **2**, the predicted U−N distances (1.860 Å) and U−I distances (3.197 Å) are also within 0.005 Å of the experimental values. Similarly, the calculated N−U−N angles were within 2° of the experimental values (173.5° for $U(NMe)_2I_2(THF)_2$ and 175.7° for complex **2**). This is in good agreement with the experimental measurements considering that the molecules were optimized in isolation and, in the case of $U(NMe)_2I_2(THF)_2$, the ligands were slightly simplified.

At the minimum energy structure the vibrational frequencies were calculated and the strong active infrared peaks from experiment identified with the calculated peaks at 1229 cm^{-1} for $U(NMe)_2I_2(THF)_2$ and 1326 cm^{-1} for complex **2**. The calculated frequencies appear shifted by the order of 70 cm^{-1} from those determined by experiment, which corresponds to the expected error of DFT for this type of calculation.[42] This identification shows that the active IR modes correspond to the N−U vibrational mode coupled out of phase with the N−C stretch mode, coupling which is expected given the closeness in mass of the nitrogen and carbon atoms.

A series of isomers of $U(NMe)_2I_2(THF)_2$ and complex **2** were also studied to quantify the energy landscape for the different possible configurations of the ligands (Figure 5). For $U(NMe)_2I_2(THF)_2$, the configuration with the two THF ligands in a trans arrangement was studied (**C**), as well as two configurations containing cis imido ligands, **D** and **E**. Complex **C** was found to have essentially the same energy as the experimentally observed isomer, while **D** and **E** were found to be 14.7 and 16.5 kcal/mol higher, respectively, demonstrating a profound energetic preference for the trans imido geometry. This energy landscape is similar to that of the uranyl-hydroxo species $UO_2(OH)_4$ where the cis uranyl is 19 kcal/mol higher than the trans

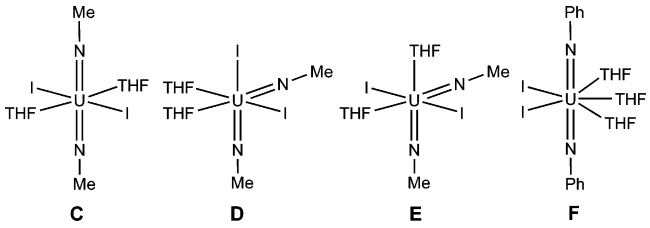

Figure 5. Isomers of $U(NMe)_2I_2(THF)_2$ and **2** studied by DFT.

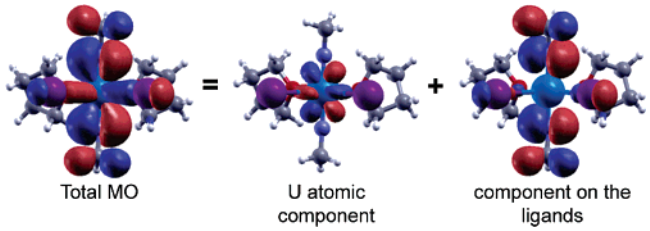

Figure 6. Decomposition of the first bonding orbital (HOMO−6) between the metal center and the nitrogen ligands. This decomposition clearly shows the molecular orbital as consisting of a $5f_\pi$ atomic orbital of the uranium forming a covalent π bond with an antibonding π orbital on the imido ligands.

species.[43] For complex **2**, a second isomer (**F**) was found to be essentially isoenergetic with the observed isomer. This species, with all three THF ligands confined to one-half of the equatorial plane, bears resemblance to complex **1a**.

The nature of the chemical bonding between the metal center and the imido ligands was analyzed for $U(NMe)_2I_2(THF)_2$ and **2** from the charge distribution and molecular orbitals, as determined by the DFT calculations. Overall, there are six orbitals with strong interactions between the uranium center and the nitrogen ligands, indicating the presence of two triple bonds analogous to the U−O bonds in the uranyl ion. Each of these six orbitals contains a strong admixture of either 5f or 6d character on the uranium, according to Mulliken population analysis. Table 1 shows the Mulliken decomposition for each of these six molecular orbitals involved in the U−N bonding. Because the highest six occupied molecular orbitals correspond to the lone pair 5p electrons of the iodide ligands, the first U−N bonding orbitals are HOMO−6 and HOMO−7. In these two molecular orbitals, the uranium participates in the bonding via the $5f_\pi$ electrons (Figure 6). The uranium 5f contributions to these MOs are 32% and 27%, respectively. In HOMO−8, the metal uses both $5f_\sigma$ (23%) and $6d_\pi$ (13%), while the metal contribution to HOMO−9 is all $6d_\pi$ in character (24%). In these four orbitals, the nitrogen contributions range from 20% to 24%. The remaining two U−N bonding orbitals were identified as HOMO−12, with a uranium component composed of $5f_\sigma$ (24%),

(41) Becke, A. D. *J. Chem. Phys.* **1993**, *98*, 5648−5652.
(42) Staroverov, V. N.; Scuseria, G. E.; Tao, J.; Perdew, J. P. *J. Chem. Phys.* **2003**, *119*, 12129−12137.
(43) Schreckenbach, G.; Hay, P. J.; Martin, R. L. *Inorg. Chem.* **1998**, *37*, 4442−4451.

Table 2. Electronic Population of the Valence Uranium Atomic Orbitals for $U(NMe)_2I_2(THF)_2$, $U(NPh)_2I_2(THF)_3$ (**2**), and UO_2^{2+}, As Determined by Mulliken and Natural Bond Orbital Analysis[a]

	$U(NMe)_2I_2(THF)_2$		**2**		UO_2^{2+}	
	Mulliken	NBO	Mulliken	NBO	Mulliken	NBO
7s	0.133	0.265	0.126	0.260	−0.073	0.035
7p	0.000	0.007	0.000	0.004	0.000	0.010
6d	2.016	1.802	1.945	1.704	1.249	0.992
5f	2.633	2.855	2.545	2.808	2.449	2.494
6p	5.737	6.000[b]	5.652	6.000[b]	5.650	6.000[b]
q_U	+1.50	+1.27	+1.73	+1.41	+2.73	+2.84

[a] The final row shows total valence charge (q_U) on uranium. For the sake of comparing UO_2^{2+} to complexes **1** and **2**, the oxygen atoms were placed 1.84 Å from the uranium center. [b] The NBO analysis puts the 6p electrons in the core.

Scheme 1

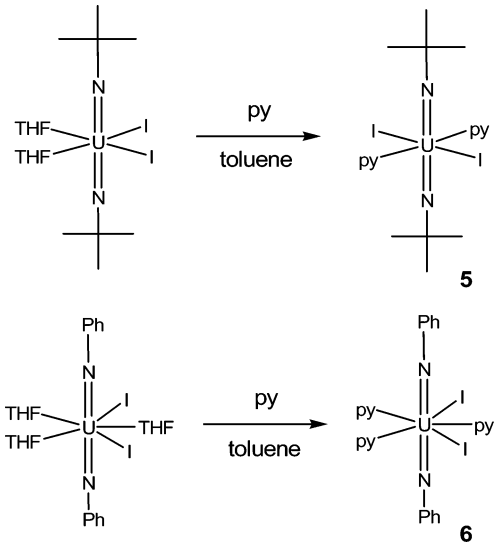

mixed in with 8% 6d and 8% p_σ, and HOMO−21, where the uranium contribution is $6d_\sigma$ (10% participation). Overall, we can say that the U−N bonding orbitals in $U(NMe)_2I_2(THF)_2$ are of the same type as those of the UO_2^{2+} fragment, which has six bonding orbitals, σ_g, σ_u, two π_u, and two π_g,[44] although the ordering is different. This difference in order is an indication that the "pushing-from-below" mechanism proposed for uranyl does not exert a strong influence in the present case due perhaps to a smaller involvement of the uranium 6p orbital in the binding MOs.

In each orbital, the uranium contribution is large, indicating a strong covalent interaction. This is consistent with the Mulliken population analysis, which assigns an effective total charge on uranium of +1.50 (Table 2). In contrast, for a completely ionic description the formal charge on U(VI) would be +6. Furthermore, the natural bond orbital (NBO) analysis assigns an effective total charge of +1.27. For comparison, an NBO analysis of the uranyl ion assigns a higher charge on uranium (+2.84), indicating a more ionic interaction. These conclusions are in agreement with those of Kaltsoyannis,[17] who carried out an extensive analysis of the six bonding orbitals in the naked UN_2 and $U(NPR_3)_2^{4+}$ fragments and found that the U−N bonds were more covalent than the analogous U−O interactions in uranyl.

Table 2 shows the total population on uranium for s, p, d, and f electrons explicitly treated in the $60e^-$ core potential. The

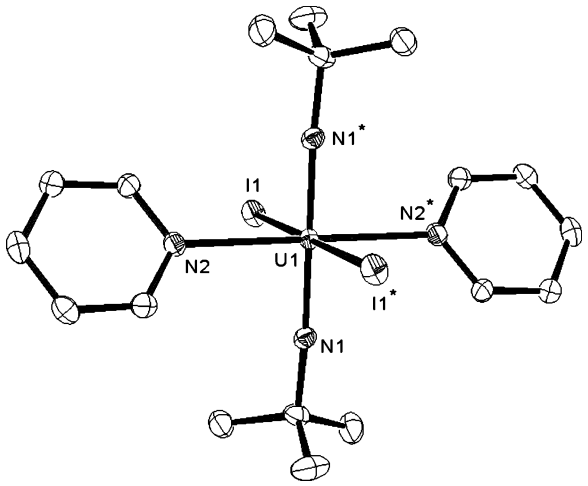

Figure 7. Solid-state molecular structure of $U(N^tBu)_2I_2(py)_2$ (**5**). Selected bond lengths (Å) and angles (deg): U1−N1 = 1.835(2), U1−N2 = 2.538(2), U1−I1 = 3.0652(2), N1−U1−N1* = 180.0(1), C1−N1−U1 = 174.5(2).

valence populations in the table are obtained by subtracting the "core" $5s^25p^65d^{10}6s^26p^6$ configurations. While the populations in $U(NMe)_2I_2(THF)_2$ and **2** are similar, the bonding in the uranyl ion shows more ionic character.

Reactivity Studies. Preliminary reactivity studies have shown that complexes **1** and **2** readily react with Lewis bases. For instance, addition of pyridine to toluene solutions of **1** provides $U(N^tBu)_2I_2(py)_2$ (**5**) in 74% yield (Scheme 1). $U(NPh)_2I_2(py)_3$ (**6**) can be generated in an analogous fashion. Complex **5** is an orange crystalline solid that is soluble in THF and toluene, while **6** is a brown microcrystalline solid that is insoluble in toluene, poorly soluble in THF, but quite soluble in CH_2Cl_2.

The solid-state molecular structure of **5** was determined by X-ray crystallography. Complex **5** crystallizes in the monoclinic space group $P2_1/c$, and its ORTEP diagram is shown in Figure 7. In contrast to **1**, complex **5** has *trans*-iodide and *trans*-THF ligands. This observation supports the theoretical calculations, which suggested that the *trans*-iodide isomer of $U(NMe)_2I_2(THF)_2$ was only slightly higher in energy than the *cis*-iodide isomer. The metrical parameters of the two *tert*-butylimido ligands are similar to those of **1**, while the comparable uranyl complex, $UO_2I_2(py)_3$, is also known.[23]

Addition of 2 equiv of Ph_3PO to **1** and **2** generates $U(N^tBu)_2I_2(Ph_3PO)_2$ (**7**) and $U(NPh)_2I_2(Ph_3PO)_2$ (**8**), respectively (eq 3). Both **7** and **8** are insoluble in toluene, poorly soluble in THF, and soluble in CH_2Cl_2. The $^{31}P\{^1H\}$ NMR spectra of **7** and **8** each exhibit a single peak at 45.5 and 49.9 ppm, respectively.

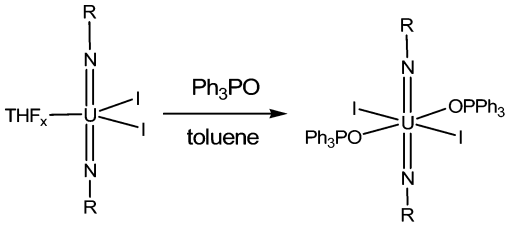

(3)

R = ^{t}Bu, x = 2; Ph, x = 3 R = ^{t}Bu, **7**; Ph, **8**

X-ray suitable crystals of **7** were grown from CH_2Cl_2/hexanes, and its solid-state molecular structure is shown in Figure 8. Consistent with the other bis(imido) complexes presented here,

(44) Pepper, M.; Bursten, B. E. *Chem. Rev.* **1991**, *91*, 719−741.

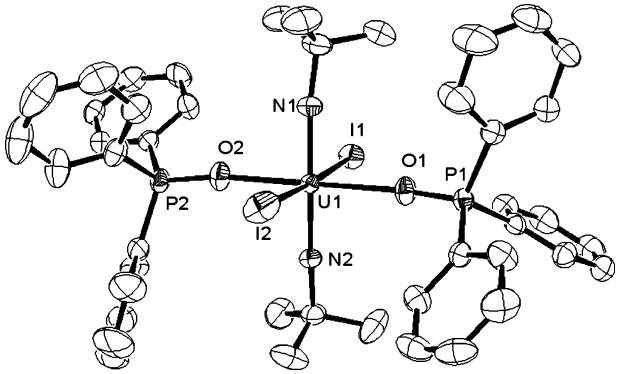

Figure 8. Solid-state molecular structure of $U(N^tBu)_2I_2(Ph_3PO)_2$ (**7**). Selected bond lengths (Å) and angles (deg): U1−N1 = 1.840(3), U1−N2 = 1.839(3), U1−O1 = 2.358(3), U1−O2 = 2.317(3), U1−I1 = 3.0928(4), U1−I2 = 3.0832(4), N1−U1−N2 = 177.8(2), C5−N2−U1 = 171.5(3), C1−N1−U1 = 170.4(3).

7 has short U−N bonds (U1−N1 = 1.840(3) Å, U1−N2 = 1.839(3) Å) and a linear N−U−N angle (177.8(2)°), while the U−O bond lengths in **7** (U1−O1 = 2.358(3) Å, U1−O2 = 2.317(3) Å) are comparable to those seen in the uranyl analogue, $UO_2I_2(Ph_3PO)_2$.[21]

The bis(imido) uranium fragment is also capable of binding PMe_3. Thus, addition of PMe_3 to **1** and **2** provides the isostructural complexes $U(N^tBu)_2I_2(PMe_3)_2(THF)$ (**9**) and $U(NPh)_2I_2(PMe_3)_2(THF)$ (**10**), respectively (eq 4).

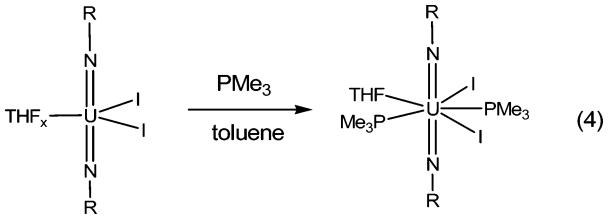

(4)

R = ^{t}Bu, x = 2; Ph, x = 3 R = ^{t}Bu, **9**; Ph, **10**

Complex **9** is an orange crystalline solid, while **10** is dark brown. The $^{31}P\{^1H\}$ NMR spectrum of **9** consists of a broad singlet at 42.1 ppm (fwhm = 900 Hz) at room temperature, while that of **10** appears at 68.2 ppm (fwhm = 480 Hz). The uranyl ion is not known to bind phosphines, so the isolation of **9** and **10** indicates that there are significant electronic differences between our bis(imido) complexes and uranyl. This suggests that the $[U(NR)_2]^{2+}$ fragment is a much softer Lewis acid than the uranyl ion, which is consistent with the DFT calculations on the two species.

Given the rarity of uranium−phosphine complexes, the solid-state molecular structure of **9** was determined by X-ray crystallography. Complex **9** was found to crystallize in the tetragonal space group $P\text{-}42_1/c$, and its solid-state molecular structure is shown in Figure 9. The metrical parameters of the bis(imido) fragment are comparable to those of **5** and **7** (U1−N1 = 1.833(6) Å, U1−N2 = 1.823(5) Å, N1−U1−N2 = 177.8(3)°), while the U−P distances in **9** (U1−P1 = 3.075(3) Å, U1−P2 = 3.042(2) Å) are comparable to the U−P bond lengths in other uranium phosphine complexes.[45] Only one other trimethylphosphine complex of uranium has been structurally characterized $(MeCp)_3U(PMe_3)$, and it has a slightly shorter U−P bond length of 2.972(6) Å.[46] All previously characterized

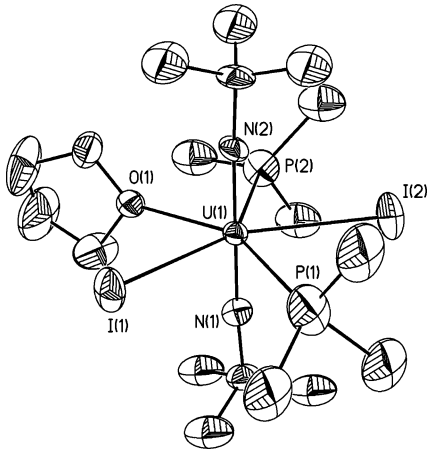

Figure 9. Solid-state molecular structure of $U(N^tBu)_2I_2(PMe_3)_2(THF)$ (**9**). Selected bond lengths (Å) and angles (deg): U1−N1 = 1.833(6), U1−N2 = 1.823(5), U1−O1 = 2.492(4), U1−I1 = 3.1402(7), U1−I2 = 3.1204(6), U1−P1 = 3.075(3), U1−P2 = 3.042(2), N1−U1−N2 = 177.8(3), C5−N1−U1 = 172.7(6), C1−N2−U1 = 176.3(6).

uranium phosphine complexes are either U(III) or U(IV), making complexes **9** and **10** the first known phosphine complexes of U(VI).

The previous paragraphs have demonstrated that the THF ligands in **1** and **2** are readily replaced with other Lewis bases. In addition to this, the iodide ligands in both **1** and **2** can undergo metathesis reactions. For instance, reaction of **1** with 2 equiv of AgOTf in CH_2Cl_2, followed by crystallization from THF/hexanes, provides $U(N^tBu)_2(OTf)_2(THF)_3$ (**11**) in moderate yields, while reaction of **2** with 2 equiv of AgOTf in CH_2Cl_2, and subsequent crystallization from CH_2Cl_2/THF/hexanes, gives $U(NPh)_2(OTf)_2(THF)_3$ (**12**) (eq 5).

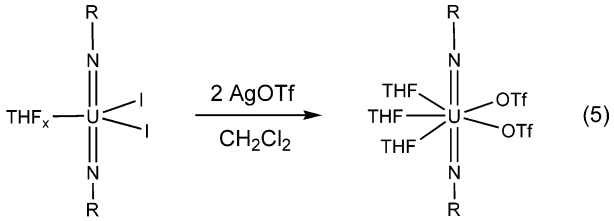

(5)

R = ^{t}Bu, x = 2; Ph, x = 3 R = ^{t}Bu, **11**; Ph, **12**

The ^1H NMR spectrum of **11** in THF-d_8 exhibits a singlet at 0.23 ppm, confirming the presence of a *tert*-butyl imido ligand, while the ^{19}F NMR spectrum exhibits a single peak at −79.3 ppm, confirming the presence of the triflate ligand. Complex **11** crystallizes in the orthorhombic space group $Pbc2_1$;[47] however, one triflate ligand is badly disordered and could not be effectively modeled. The X-ray data do confirm the proposed connectivity though, which is isostructural with **1a**.

The ^1H NMR spectrum of **12** in CD_2Cl_2 exhibits several broad resonances at room temperature. Cooling a CD_2Cl_2 solution of **12** to −40 °C provides a spectrum with much sharper resonances. By ^1H NMR, complex **12** contains three THF ligands in two different environments, in addition to two phenyl groups. Only one resonance is observed in the ^{19}F NMR spectrum, at

(45) Edwards, P. G.; Andersen, R. A.; Zalkin, A. *J. Am. Chem. Soc.* **1981**, *103*, 7792−7794.
(46) Brennan, J. G.; Zalkin, A. *Acta Crystallogr., Sect. C* **1985**, *41*, 1038−1040.
(47) Crystal data for $U(N^tBu)_2(OTf)_2(THF)_3$ (**11**): orthorhombic, $Pbc2_1$, a = 11.946(5) Å, b = 16.145(6) Å, c = 17.315(7) Å, V = 3340(2) Å^3, Z = 8.

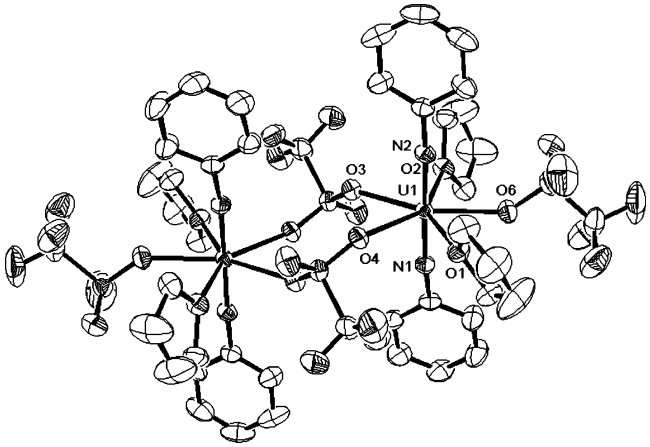

Figure 10. Solid-state molecular structure of $[U(NPh)_2(OTf)_2(THF)_2]_2 \cdot 2CH_2Cl_2$. CH_2Cl_2 molecules omitted for clarity. Selected bond lengths (Å) and angles (deg): U1−N1 = 1.849(3), U1−N2 = 1.847(3), U1−O6 = 2.393(3), U1−O2 = 2.400(3), U1−O1 = 2.434(3), U1−O3 = 2.459(3), U1−O4 = 2.463(3), N1−U1−N2 = 177.7(2), C1−N1−U1 = 172.2(3), C7−N2−U1 = 175.2(3).

−79.0 ppm. Given this, there are two possible arrangements of the THF ligands: one in which all three THF ligands occupy one-half of the equatorial plane (as in **1a**), or one in which the third THF ligand occupies the site between the two iodide ligands (as in **2**). Because the low-temperature NMR data cannot rule out either isomer, the structure of **12** has been determined by X-ray crystallography.

X-ray quality crystals of **12** were grown slowly from a CH_2Cl_2/hexanes solution at −35 °C. Under these conditions, **12** was found to crystallize in the monoclinic space group $P2_1/n$ as a dimer. Its solid-state molecular structure is shown in Figure 10.

Like the other structurally characterized bis(imido) complexes, $[U(NPh)_2(OTf)_2(THF)_2]_2 \cdot 2CH_2Cl_2$ exhibits a trans arrangement of the two imido groups and short U−N bonds (U1−N1 = 1.849(3) Å, U1−N2 = 1.847(3) Å). Of the two triflate ligands, the nonbridging triflate has a shorter U−O contact (U1−O6 = 2.393(3) Å) than the bridging triflate (O3 = 2.459(3) Å, U1−O4 = 2.463(3) Å). The solid-state molecular structure contrasts with the analytical data, which suggest that **12** is a monomer (that is, a tris(THF) adduct) when it is isolated from solutions containing THF. In support of this, the NMR data are wholly consistent with the presence of three THF ligands. However, in THF-deficient environments, it can exist as a dimer, at least in the solid state.

Summary

In this contribution, we have described the synthesis of several complexes with the general formula $U(NR)_2I_2(THF)_x$ (R = alkyl, aryl; x = 2, 3). Their successful synthesis leads us to believe that many different bis(imido) complexes could be synthesized via eq 2, and we are trying to extend this methodology to new bis(imido) complexes with bulky substituents attached to the nitrogen. This will allow exceptional steric and electronic control of reactivity at the metal center through the variation of the imido substituents. The DFT calculations show that the U−N interaction is a triple bond and is similar to U−O interaction in the UO_2^{2+}. The uranium atomic orbitals involved in these bonds are the $5f_\sigma$, $5f_\pi$, $6d_\pi$, and $6d_\sigma$, which is also the case in UO_2^{2+}. However, the bonding in the bis(imido) fragment is more covalent in character. In addition, complexes **1** and **2** have proven to be excellent starting materials for the synthesis of new uranium imido complexes as the THF ligands in **1** and **2** are readily displaced by addition of donor ligands. Furthermore, the isolation of complexes **11** and **12** also demonstrates that the iodide ligands in **1** and **2** can undergo metathesis. This raises the possibility of synthesizing alkoxide, amide, and alkyl complexes containing the bis(imido) moiety.

Experimental Section

General. All reactions and subsequent manipulations were performed under anaerobic and anhydrous conditions under either high vacuum or an atmosphere of helium or argon. Hexanes, THF, and toluene were dried by passage over activated alumina. C_6D_6 and *tert*-butylamine were dried over activated 4 Å molecular sieves for 24 h before use. Aniline was distilled from CaH_2, while NEt_3 was distilled from Na/benzophenone. $UI_3(THF)_4$ was synthesized by the published procedure.[36] All other reagents were purchased from commercial suppliers and used as received.

NMR spectra were recorded on a Bruker AVA300. ^1H and $^{13}C\{^1H\}$ NMR spectra were referenced to the residual protio solvent peaks as internal standards (^1H NMR experiments) or the characteristic resonances of the solvent nuclei (^{13}C NMR experiments) and are reported relative to TMS. IR spectra were obtained on a Nicolet Magna-IR 560 spectrometer, while UV−vis spectra were recorded on a Varian Cary 6000i. Elemental analyses were performed at the UC Berkeley Microanalytical Facility, on a Perkin-Elmer Series II 2400 CHNS analyzer.

$U(N^tBu)_2I_2(THF)_2$. Method A. To a stirring THF solution (10 mL) containing uranium metal turnings (0.303 g, 1.27 mmol) and *tert*-butylamine (0.614 g, 8.40 mmol) was added I_2 (0.970 g, 3.82 mmol). After 2 h, the metal was consumed and the volatiles were removed in vacuo to give an orange powder. This material was washed with hexanes (10 mL) and then dissolved in toluene (15 mL). The resulting orange solution was filtered through a Celite column, and the column was rinsed with another aliquot of toluene (10 mL). The combined filtrates were layered with hexanes (15 mL), and this solution was stored at −32 °C for 24 h, resulting in the precipitation of red crystals, which were collected by decanting the supernatant. Another crop of crystals was harvested from the mother liquor, giving a total of 0.674 g, 68% yield. Anal. Calcd for $C_{16}H_{34}UI_2N_2O_2$: C, 24.69; H, 4.40; N, 3.60. Found: C, 24.64; H, 4.27; N, 3.52. ^1H NMR (C_6D_6, 25 °C, 300 MHz): δ 0.66 (s, 18H), 1.54 (br s, 8H), 4.56 (br s, 8H). $^{13}C\{^1H\}$ NMR (C_6D_6, 25 °C, 75 MHz): δ 26.1 (OCH_2CH_2), 35.9 (CH_3), 74.3 (OCH_2CH_2), 77.1 (CMe_3). IR (Nujol mull): 861 (m), 924 (w), 1010 (m), 1080 (s), 1110 (m), 1170 (s), 1220 (m), 1290 (w). UV/vis (THF, 1.2×10^{-5} M): 291 nm (ϵ = 3500 L mol^{-1} cm^{-1}), and 353 nm (ϵ = 2200 L mol^{-1} cm^{-1}).

Method B. To a purple solution of $UI_3(THF)_4$ (0.480 g, 0.53 mmol) and *tert*-butylamine (0.264 g, 3.62 mmol) in THF (10 mL) was added I_2 (0.204 g, 0.81 mmol). The solution, which quickly turned orange-red, was vigorously shaken. After 10 min, the volatiles were removed in vacuo and the resulting red oil was dissolved in toluene (10 mL). This solution was filtered though a Celite column supported on glass wool. The Celite column was rinsed with more toluene (5 mL), and the combined filtrates were layered with an equal volume of hexanes and stored at −32 °C for 72 h, resulting in the precipitation of red crystals, which were collected by decanting the supernatant. 0.362 g, 87% yield.

$U(NPh)_2I_2(THF)_3$. I_2 (0.372 g, 1.47 mmol) was added to a purple solution of $UI_3(THF)_4$ (0.898 g, 0.99 mmol), aniline (0.194 g, 2.09 mmol), and NEt_3 (0.509 g, 5.03 mmol) dissolved in THF (15 mL). The solution turned orange-red, and a white crystalline precipitate quickly formed. The solution was shaken for 10 min at which point it was stored at −35 °C for 2 h. The cold solution was filtered through a Celite column, and the white solid was rinsed with several aliquots

of toluene (50 mL total). The volume of the combined filtrates was reduced in vacuo, and the solution was then layered with an equal volume of hexanes. The flask was then stored at −35 °C for 72 h, resulting in the precipitation of red-brown crystals, which were collected by decanting off the supernatant. 0.742 g, 84% yield. Anal. Calcd for $C_{24}H_{34}UI_2N_2O_3$: C, 32.38; H, 3.85; N, 3.15. Found: C, 31.45; H, 3.88; N, 3.15. ^{1}H NMR (C_6D_6, 25 °C, 300 MHz): δ 1.41 (m, 12H, OCH_2CH_2), 4.38 (m, 12H, OCH_2CH_2), 5.73 (t, J_{HH} = 7.4 Hz, 2H, para C−H), 6.20 (d, J_{HH} = 7.5 Hz, 4H, ortho C−H), 7.00 (t, J_{HH} = 7.8 Hz, 4H, meta C−H). ^{13}C{^{1}H} NMR (C_6D_6, 25 °C, 75 MHz): δ 26.2 (OCH_2CH_2), 70.9 (OCH_2CH_2), 125.9 (meta C), 128.9 (para C), 130.3 (ortho C), 153.7 (ipso C). IR (Nujol mull): 768 (m), 866 (m), 910 (w), 920 (w), 962 (m), 999 (w), 1020 (m), 1060 (w), 1170 (w), 1270 (br s), 1300 (w), 1340 (w), 1380 (m). UV/vis (THF, 6.8×10^{-6} M): 291 nm (ϵ = 7900 L mol^{-1} cm^{-1}), and 352 nm (ϵ = 1900 L mol^{-1} cm^{-1}).

U(N-3,5-(CF$_3$)$_2$C$_6$H$_3$)$_2$I$_2$(THF)$_3$. To a purple solution of $UI_3(THF)_4$ (0.212 g, 0.23 mmol), NEt_3 (0.168 g, 1.7 mmol), and 3,5-$(CF_3)_2C_6H_3NH_2$ (0.132 g, 0.58 mmol) in THF (5 mL) was added I_2 (0.0885 g, 0.35 mmol). The solution turned deep red, and a white crystalline precipitate quickly formed. After 10 min, the volume of the solution was reduced in vacuo to 2 mL, and the solution was stored at −35 °C for 2 h. The cold solution was filtered through a Celite column, and the white solid was rinsed with several aliquots of toluene (5 mL total). The volume of the combined filtrates was reduced in vacuo, and the solution was then layered with an equal volume of hexanes. The vial was then stored at −35 °C for 24 h, resulting in the precipitation of more white crystals. This solution was filtered through a Celite column, the volume was reduced to 2 mL in vacuo, and more hexanes were layered on top of the filtrate. Storing this vial at −35 °C for 24 h resulted in the deposition of red crystals (0.184 g, 68% yield). Anal. Calcd for $C_{28}H_{30}F_{12}I_2N_2O_3U$: C, 28.93; H, 2.60; N, 2.41. Found: C, 28.65; H, 2.36; N, 2.55. ^{1}H NMR (C_6D_6, 25 °C, 300 MHz): δ 0.45 (s, 12H, OCH_2CH_2), 2.37 (m, 12H, OCH_2CH_2), 6.54 (s, 2H, para CH), 6.75 (s, 4H, ortho CH). ^{19}F NMR (C_6D_6, 25 °C, 282 MHz): δ −64.0. ^{13}C{^{1}H} NMR (C_6D_6, 25 °C, 75 MHz): δ 25.1 (OCH_2CH_2), 70.4 (OCH_2CH_2), 121.4 (para C), 126.4 (meta C), 129.8 (q, CF_3, J_{CF} = 32 Hz), 131.1 (ortho C), 151.2 (ipso C).

U(N-2,6-(^{i}Pr)$_2$C$_6$H$_3$)$_2$I$_2$(THF)$_3$. To a purple solution of $UI_3(THF)_4$ (0.2344 g, 0.26 mmol), NEt_3 (0.104 g, 1.03 mmol), and 2,6-$(^iPr)_2C_6H_3NH_2$ (0.0986 g, 0.56 mmol) in THF (5 mL) was added I_2 (0.0980 g, 0.39 mmol). The solution, which quickly turned deep red, was vigorously shaken. No precipitate formed. The volume of the solution was reduced by one-half in vacuo, and the solution was stored at −35 °C for 2 h, resulting in the deposition of white crystals. This solution was then filtered through a column of Celite, layered with an equal volume of hexanes, and stored at −35 °C for 24 h, resulting in the deposition of brown crystals (0.046 g). Removal of all of the solvent from the supernatant and recrystallization of the resulting solid from toluene allowed for the isolation of three more crops of crystals (total yield from all crops: 0.142 g, 52%). Anal. Calcd for $C_{36}H_{58}I_2N_2O_3U$: C, 40.84; H, 5.52; N, 2.65. Found: C, 39.46; H, 5.01; N, 2.69. ^{1}H NMR (CD_2Cl_2, 25 °C, 300 MHz): δ 1.14 (d, J_{HH} = 11 Hz, 24H, Me), 1.96 (br s, 12H, OCH_2CH_2), 3.98 (br s, 4H, $CHMe_2$), 4.40 (br s, 12H, OCH_2CH_2), 5.50 (t, J_{HH} = 8 Hz, 2H, para CH), 6.97 (d, J_{HH} = 8 Hz, 4H, meta CH). ^{1}H NMR (THF-d_8, 25 °C, 300 MHz): δ 1.26 (d, J_{HH} = 7 Hz, 24H, Me), 4.27 (septet, J_{HH} = 7, 4H, $CHMe_2$), 5.50 (t, J_{HH} = 8 Hz, 2H, para CH), 7.01 (d, J_{HH} = 8 Hz, 4H, meta CH). ^{13}C{^{1}H} NMR (THF-d_8, 25 °C, 75 MHz): δ 26.8 ($CHMe_2$), 28.1 (Me), 119.8 (meta C), 129.3 (para C), 138.6 (ortho C), 151.4 (ipso C).

U(N^{t}Bu)$_2$I$_2$(py)$_2$. To an orange solution of $U(N^tBu)_2I_2(THF)_2$ (0.112 g, 0.14 mmol) in toluene (5 mL) was added pyridine (0.101 g, 1.28 mmol). This solution was filtered through a Celite column and then layered with an equal volume of hexanes. The solution was then stored at −35 °C for 24 h, resulting in the precipitation of orange crystals, which were collected by decanting off the supernatant (0.0846 g, 74% yield). Anal. Calcd for $C_{18}H_{28}UI_2N_4$: C, 27.29; H, 3.56; N, 7.07. Found: C, 27.29; H, 3.79; N, 6.94. ^{1}H NMR (THF-d_8, 25 °C, 300 MHz): δ 0.49 (s, 18H, CMe_3), 7.43 (t, 4H, J_{HH} = 12 Hz, CH), 7.79 (t, 2H, J_{HH} = 8 Hz, CH), 8.93 (br, 4H, CH). ^{13}C{^{1}H} NMR (THF-d_8, 25 °C, 75 MHz): δ 35.7 (CMe_3), 77.0 (CMe_3), 124.9 (CH), 137.4 (CH), 151.1 (CH).

U(NPh)$_2$I$_2$(py)$_3$. To a Et_2O (2 mL) and toluene (2 mL) solution of $U(NPh)_2I_2(THF)_3$ (0.0796 g, 0.09 mmol) was added pyridine (0.149 g, 1.89 mmol). The vial was then stored at −35 °C for 24 h, resulting in the precipitation of red-brown crystals, which were collected by decanting off the supernatant (0.0413 g, 51%). Anal. Calcd for $C_{27}H_{25}UI_2N_5$: C, 35.58; H, 2.76; N, 7.68. Found: C, 34.20; H, 2.69; N, 7.28. ^{1}H NMR (THF-d_8, 25 °C, 300 MHz): δ 5.74 (d, 4H, J_{HH} = 7 Hz, imido ortho CH), 5.82 (t, 2H, J_{HH} = 7 Hz, imido para CH), 6.96 (t, 4H, J_{HH} = 8 Hz, imido meta CH), 7.31 (m, 6H, py meta CH), 7.71 (t, 3H, J_{HH} = 8 Hz, py para CH), 8.63 (d, 6H, J_{HH} = 4 Hz, py ortho CH). ^{13}C{^{1}H} NMR (THF-d_8, 25 °C, 75 MHz): δ 124.6 (py meta CH), 125.8 (imido meta CH), 128.5 (imido para CH), 130.5 (imido ortho CH), 136.8 (py para CH), 151.1 (py ortho CH), 153.7 (imido ipso C).

U(N^{t}Bu)$_2$I$_2$(Ph$_3$PO)$_2$. To an orange solution of $U(N^tBu)_2I_2(THF)_2$ (0.0661 g, 0.08 mmol) in toluene (5 mL) was added Ph_3PO (0.0496 g, 0.18 mmol), also dissolved in toluene (2 mL). After 2 h, large orange crystals had been deposited in the vial, and the supernatant was almost colorless. The crystals were isolated by decanting the solvent (0.0728 g, 72% yield). Anal. Calcd for $C_{44}H_{48}UI_2N_2O_2P_2$: C, 44.39; H, 4.06; N, 2.35. Found: C, 44.58; H, 4.0; N, 2.24. ^{1}H NMR (CD_2Cl_2, 25 °C, 300 MHz): δ 0.01 (s, 18H, CMe_3), 7.66 (m, 18H, CH), 8.39 (m, 12H, CH). ^{31}P{^{1}H} NMR (CD_2Cl_2, 25 °C, 121 MHz): δ 45.5. ^{13}C{^{1}H} NMR (CD_2Cl_2, 25 °C, 75 MHz): δ 34.9 (CMe_3), 64.4 (CMe_3), 129.2 (d, J_{CP} = 14 Hz, CH), 133.6 (s, CH), 134.1 (d, J_{CP} = 11 Hz, CH).

U(NPh)$_2$I$_2$(Ph$_3$PO)$_2$·C$_7$H$_8$. To a brown-orange solution of $U(NPh)_2I_2(THF)_3$ (0.0823 g, 0.09 mmol) in toluene (5 mL) was added Ph_3PO (0.0530 g, 0.19 mmol), also dissolved in toluene (2 mL). After 5 min, black crystals had begun to form. The vial was stored at −35 °C for 24 h, resulting in the further precipitation of crystals, which were collected by decanting the supernatant (0.0698 g, 57% yield). Anal. Calcd for $C_{48}H_{40}UI_2N_2O_2P_2·C_7H_8$: C, 49.94; H, 3.66; N, 2.13. Found: C, 49.86; H, 3.48; N, 2.08. ^{1}H NMR (CD_2Cl_2, 25 °C, 300 MHz): 5.17 (d, 4H, J_{HH} = 8 Hz, imido ortho CH), 5.69 (t, 2H, J_{HH} = 7 Hz, imido para CH), 6.94 (t, 4H, J_{HH} = 8 Hz, imido meta CH), 7.40 (m, 12H, meta CH), 7.60 (t, 6H, J_{HH} = 8 Hz, para CH), 8.09 (dd, 12H, J_{HH} = 8 Hz, J_{HP} = 13 Hz, ortho CH). ^{31}P{^{1}H} NMR (CD_2Cl_2, 25 °C, 121 MHz): δ 49.9. ^{13}C{^{1}H} NMR (CD_2Cl_2, 25 °C, 75 MHz): δ 125.5 (imido meta CH), 127.4 (imido para CH), 129.9 (s, J_{CP} = 13 Hz, meta CH), 130.2 (d, J_{CP} = 14 Hz, ispo C), 130.4 (imido ortho CH), 134.4 (para CH), 134.5 (d, J_{CP} = 11 Hz, ortho CH), 153.0 (imido ipso C).

U(N^{t}Bu)$_2$I$_2$(PMe$_3$)$_2$(THF). To an orange solution of $U(N^tBu)_2I_2(THF)_2$ (0.0776 g, 0.10 mmol) in toluene (5 mL) was added PMe_3 (0.0560 g, 0.74 mmol). The solution was then filtered through a Celite column, and an equal volume of hexanes was layered onto the supernatant. The vial was stored at −35 °C for 24 h, resulting in the precipitation of crystals, which were collected by decanting off the supernatant (0.0521 g, 61%). Anal. Calcd for $C_{18}H_{44}I_2N_2OP_2U$: C, 25.19; H, 5.17; N, 3.26. Found: C, 25.27; H, 5.18; N, 3.37. ^{1}H NMR (C_6D_6, 25 °C, 300 MHz): δ 0.71 (s, 18H, CMe_3), 1.48 (m, 22H, PMe_3 and OCH_2CH_2), 4.09 (s, 4H, OCH_2CH_2). ^{31}P{^{1}H} NMR (C_6D_6, 25 °C, 121 MHz): δ 42.1 (fwhm = 900 Hz). ^{13}C{^{1}H} NMR (C_6D_6, 25 °C, 75 MHz): δ 18.4 (br s, PMe_3), 26.1 (OCH_2CH_2), 36.6 (CMe_3), 71.5 (OCH_2CH_2), 77.4 (CMe_3).

U(NPh)$_2$I$_2$(PMe$_3$)$_2$(THF). To an orange-brown solution of $U(NPh)_2I_2(THF)_3$ (0.0843 g, 0.09 mmol) in toluene (5 mL) was added PMe_3 (0.060 g, 0.79 mmol). The solution was then filtered through a Celite column, and an equal volume of hexanes was layered onto the supernatant. The vial was stored at −35 °C for 24 h, resulting in the precipitation of crystals, which were collected by decanting off the supernatant (0.0463 g, 54%). Anal. Calcd for $C_{22}H_{36}I_2N_2OP_2U$: C, 29.41; H, 4.04; N, 3.12.

Table 3. X-ray Crystallographic Data for Complexes **1**−**3**

crystal data	**1**	**1a**	**2**	**3**
empirical formula	$C_{16}H_{34}I_2N_2O_2U$	$C_{22}H_{42}I_2N_2O_3U$	$C_{24}H_{34}N_2I_2O_3U$	$C_{28}H_{30}F_{12}I_2N_2O_3U$
crystal habit, color	block, orange	irregular, red	block, red	plate, red
crystal size (mm)	0.12 × 0.08 × 0.08	0.16 × 0.14 × 0.12	0.30 × 0.22 × 0.12	0.22 × 0.148 × 0.01
crystal system	monoclinic	monoclinic	monoclinic	orthorhombic
space group	$P2_1/n$	$C2/c$	$P2_1/n$	$Pbc2_1$
volume (Å^3)	2373.7(2)	2670.7(2)	2772.0(4)	6899.0(8)
a (Å)	12.3751(7)	11.7556(5)	10.9867(8)	9.1025(6)
b (Å)	15.3700(8)	13.8565(6)	17.7376(13)	17.488(1)
c (Å)	12.4804(7)	17.1139(9)	14.2243(11)	43.339(3)
α (°)	90	90	90	90
β (°)	90.507(1)	106.660(1)	90.070(1)	90
γ (°)	90	90	90	90
Z	4	4	4	8
formula weight (g/mol)	778.28	874.41	890.36	1162.37
density (calcd) (M g/m^3)	2.178	2.175	2.133	2.238
absorption coefficient (cm^{-1})	9.448	8.414	8.109	6.593
F_{000}	1432	1640	1656	4336
radiation	Mo Kα, 0.71073 Å	Mo Kα, 0.71073 Å	Mo Kα, 0.71073 Å	Mo Kα, 0.71073 Å
data refinement				
final R indices[a]	$R_1 = 0.029$, w$R_2 = 0.061$	$R_1 = 0.017$, $R_2 = 0.042$	$R_1 = 0.018$, w$R_2 = 0.042$	$R_1 = 0.034$, $R_2 = 0.084$
largest diff. peak and hole (e Å^{-3})	2.70 and −0.74	0.71 and −0.63	1.03 and −0.54	1.18 and −1.12

[a] Number of observed reflections: **1**, 5822 ($I_o > 2\sigma I_o$), R1 = $\sum(|F_o| - |F_c|)/\sum|F_o|$, wR2 = $[\sum w(|F_o|^2 - |F_c|^2)^2/\sum wF_o^4]^{1/2}$, $w = [\sigma^2F_o^2 + (0.0215p)^2 + 2.1893p]^{-1}$, $p = [F_o^2 + 2F_c^2]/3$. **1a**, 3075 ($I_o > 2\sigma I_o$), R1 = $\sum(|F_o| - |F_c|)/\sum|F_o|$, wR2 = $[\sum w(|F_o|^2 - |F_c|^2)^2/\sum wF_o^4]^{1/2}$, $w = [\sigma^2F_o^2 + (0.0215p)^2]^{-1}$, $p = [F_o^2 + 2F_c^2]/3$. **2**, 6802 ($I_o > 2\sigma I_o$), R1 = $\sum(|F_o| - |F_c|)/\sum|F_o|$, wR2 = $[\sum w(|F_o|^2 - |F_c|^2)^2/\sum wF_o^4]^{1/2}$, $w = [\sigma^2F_o^2 + (0.0188p)^2 + 0.6614p]^{-1}$, $p = [F_o^2 + 2F_c^2]/3$. **3**, 9694 ($I_o > 2\sigma I_o$), R1 = $\sum(|F_o| - |F_c|)/\sum|F_o|$, wR2 = $[\sum w(|F_o|^2 - |F_c|^2)^2/\sum wF_o^4]^{1/2}$, $w = [\sigma^2F_o^2 + (0.0145p)^2 + 149.7929p]^{-1}$, $p = [F_o^2 + 2F_c^2]/3$.

Found: C, 28.14; H, 3.79; N, 2.81. ^{1}H NMR (C_6D_6, 25 °C, 300 MHz): δ 1.55 (s, 4H, OCH$_2$C*H*$_2$), 1.61 (s, 18H, PMe$_3$), 4.50 (s, 4H, OC*H*$_2$-CH$_2$), 5.71 (t, $J_{HH} = 7$ Hz, 2H, para CH), 6.17 (d, $J_{HH} = 8$ Hz, 4H, ortho CH), 7.04 (t, $J_{HH} = 8$ Hz, 4H, meta CH). ^{31}P{^{1}H} NMR (C_6D_6, 25 °C, 121 MHz): δ 68.2 (fwhm = 480 Hz). ^{13}C{^{1}H} NMR (C_6D_6, 25 °C, 75 MHz): δ 18.5 (br s, PMe$_3$), 26.2 (OCH$_2$C*H*$_2$), 74.2 (O*C*H$_2$-CH$_2$), 125.8 (para CH), 129.7 (meta CH), 130.8 (ortho CH), 153.8 (ipso CH).

U(N^{t}Bu)$_2$(OTf)$_2$(THF)$_3$. To an orange solution of U(N^{t}Bu)$_2$I$_2$(THF)$_2$ (0.192 g, 0.25 mmol) in CH_2Cl_2 (5 mL) was added AgOTf (0.1273 g, 0.50 mmol). After 2 h of stirring, the volatiles were removed in vacuo and the resulting orange solid was dissolved in a mixture of THF (3 mL) and MeCN (1 mL). This solution was filtered through a Celite column, and the column was rinsed with THF (1 mL). Hexanes (4 mL) were layered on top of the filtrate, and the vial was stored at −35 °C for 24 h, resulting in the precipitation of fine white crystals. The orange supernatant was decanted from the crystals, and the volatiles were removed to give an orange oil. This was dissolved in THF (1 mL), and the resulting orange solution was layer with hexanes (1 mL) and stored at −35 °C for 7 days, resulting in the deposition of orange blocks (0.0537 g, 24% yield). Upon application of vacuum, the orange crystals slowly crumbled and turned opaque. Anal. Calcd for $C_{22}H_{42}F_6N_2O_9S_2U$: C, 29.53; H, 4.73; N, 3.13. Found: C, 26.76; H, 4.16; N, 3.52 (analysis is consistent with U(N^{t}Bu)$_2$(OTf)$_2$(THF)$_2$; Anal. Calcd for $C_{18}H_{34}F_6N_2O_8S_2U$: C, 26.28; H, 4.17; N, 3.41). ^{1}H NMR (THF-d_8, 25 °C, 300 MHz): δ 0.23 (s, 18H, CMe$_3$), 1.70 (m, OCH$_2$C*H*$_2$), 3.61 (m, OC*H*$_2$CH$_2$). ^{19}F NMR (THF-d_8, 25 °C, 282 MHz): δ −79.3. ^{13}C{^{1}H} NMR (THF-d_8, 25 °C, 75 MHz): δ 26.5 (OCH$_2$C*H*$_2$), 35.3 (C*Me*$_3$), 68.4 (OCH$_2$CH$_2$), 81.2 (*C*Me$_3$).

U(NPh)$_2$(OTf)$_2$(THF)$_3$. To an orange-brown solution of U(NPh)$_2$I$_2$-(THF)$_3$ (0.2085 g, 0.24 mmol) in CH_2Cl_2 (2 mL) was added AgOTf (0.1206 g, 0.47 mmol). After 2 h of stirring, this solution was filtered through a Celite column and the column was rinsed with THF (2 mL). Hexanes (4 mL) were layered on top of the filtrate, and the vial was stored at −35 °C for 24 h, resulting in the precipitation of fine maroon-brown crystals (0.1109 g, 51% yield). Anal. Calcd for $C_{26}H_{34}$-$F_6N_2O_9S_2U$: C, 33.41; H, 3.67; N, 3.00. Found: C, 33.34; H, 3.61; N, 2.98. ^{1}H NMR (CD_2Cl_2, −40 °C, 300 MHz): δ 2.36 (s, 4H, OCH$_2$C*H*$_2$), 2.54 (s, 4H, OCH$_2$C*H*$_2$), 4.89 (s, 8H, OC*H*$_2$CH$_2$), 5.10 (m, 12H, ortho CH and OC*H*$_2$CH$_2$), 5.80 (t, $J_{HH} = 7$ Hz, 2H, para CH), 7.03 (t, $J_{HH} = 8$ Hz, 4H, meta CH). ^{19}F NMR (CD_2Cl_2, −40 °C, 282 MHz): δ −79.0. ^{13}C{^{1}H} NMR (CD_2Cl_2, −40 °C, 75 MHz): δ 26.6 (OCH$_2$C*H*$_2$), 26.7 (OCH$_2$C*H*$_2$), 75.2 (O*C*H$_2$CH$_2$), 76.5 (O*C*H$_2$CH$_2$), 125.1 (CH), 127.9 (CH), 129.0 (CH), 153.6 (ipso CH).

X-ray Crystallography. The data for **1**, **1a**, **2**, **3**, **4**, and **5** were collected on a Bruker X-ray diffractometer, with a D8 goniometer and an APEX II charge-coupled-device (CCD) detector. The crystal was cooled with a KRYO-FLEX liquid nitrogen vapor cooling device to 141 K. The instrument was equipped with a graphite monochromatized Mo Kα X-ray source ($\lambda = 0.71073$ Å), with MonoCap X-ray source optics. A hemisphere of data was collected using ω scans, with 5-s frame exposures and 0.3° frame widths. Data collection and initial indexing and cell refinement were handled using APEX II software.[48] Frame integration, including Lorentz-polarization corrections, and final cell parameter calculations were carried out using SAINT+ software.[49] The data were corrected for absorption using the SADABS program.[50] Decay of reflection intensity was monitored via analysis of redundant frames.

The data for **7** and **12** were collected on a Bruker P4/1k-CCD diffractometer and cooled to 203 K using a Bruker LT-2 temperature device. The instrument was equipped with a sealed, graphite monochromatized Mo Kα X-ray source ($\lambda = 0.71073$ Å). A hemisphere of data was collected using φ scans, with 30 s frame exposures and 0.3° frame widths. Data collection and initial indexing and cell refinement were handled using SMART software.[51] Frame integration, including Lorentz-polarization corrections, and final cell parameter calculations were carried out using SAINT.[52] Decay of reflection intensity was monitored via analysis of redundant frames.

The structures were solved using direct methods and difference Fourier techniques. All hydrogen atom positions were idealized and rode on the atom they were attached to. For all compounds, the final refinement included anisotropic temperature factors on all non-hydrogen atoms. Structures **1**, **4**, and **9** had ligand disorder (^{t}Bu group for **1**, THF for **4**, and PMe$_3$ and ^{t}Bu for **9**) that was modeled as two one-half occupancy positions. Lattice solvent molecules for **4** (THF) and **12** (dichloromethane) were found and refined anisotropically, with hydrogen atoms. Structure solution, refinement, graphics, and creation of publication materials were performed using SHELXTL.[53] A summary

(48) *APEX II 1.08*; Bruker AXS, Inc.: Madison, WI, 2004.
(49) *SAINT+ 7.06*; Bruker AXS, Inc.: Madison, WI, 2003.
(50) Sheldrick, G. M. *SADABS 2.03*; University of Göttingen: Germany, 2001.
(51) *SMART 5.054*; Bruker AXS, Inc.: Madison, WI, 1996.
(52) *SAINT 6.45A*; Bruker AXS, Inc.: Madison, WI, 2003.
(53) *SHELXTL 5.10*; Bruker AXS, Inc.: Madison, WI, 1997.

Table 4. X-ray Crystallographic Data for Complexes **4**·THF−**9**

crystal data	**4**·THF	**5**	**7**	**9**
empirical formula	$C_{36}H_{58}I_2N_2O_3U{\cdot}OC_4H_8$	$C_{18}H_{28}I_2N_4U$	$C_{44}H_{48}N_2I_2O_2P_2U$	$C_{18}H_{44}I_2N_2OP_2U$
crystal habit, color	block, brown	block, orange	block, orange	irregular, orange
crystal size (mm)	0.14 × 0.12 × 0.08	0.14 × 0.11 × 0.04	0.30 × 0.20 × 0.10	0.20 × 0.12 × 0.10
crystal system	monoclinic	monoclinic	monoclinic	tetragonal
space group	$P2_1/c$	$P2_1/c$	$P2_1/c$	$P\text{-}42_1/c$
volume (Å^3)	4264.5(3)	1197.3(2)	4485.2(9)	5872(1)
a (Å)	16.6844(6)	8.2887(7)	11.792(1)	23.516(3)
b (Å)	13.7864(5)	15.640(1)	20.984(3)	23.516
c (Å)	18.5403(7)	9.7391(8)	18.416(2)	10.617(1)
α (°)	90	90	90	90
β (°)	90.311(1)	108.495(1)	100.172(2)	90
γ (°)	90	90	90	90
Z	4	2	4	8
formula weight (g/mol)	1130.78	792.27	1190.61	858.32
density (calcd) (M g/m^3)	1.761	2.198	1.763	1.942
absorption coefficient (cm^{-1})	5.293	9.365	5.103	7.751
F_{000}	2200	724	2280	3216
radiation	Mo Kα, 0.71073 Å	Mo Kα, 0.71073 Å	Mo Kα, 0.71073 Å	Mo Kα, 0.71073 Å
data refinement				
final *R* indices[a]	$R_1 = 0.029$, $R_2 = 0.064$	$R_1 = 0.017$, w$R_2 = 0.037$	$R_1 = 0.026$, w$R_2 = 0.048$	$R_1 = 0.034$, w$R_2 = 0.075$
largest diff. peak and hole (e Å^{-3})	2.16 and −0.77	0.63 and −0.47	0.68 and −0.53	1.49 and −0.89

[a] Number of observed reflections: **4**, 8272 ($I_o > 2\sigma I_o$), R1 = $\sum(||F_o| - |F_c||)/\sum|F_o|$, wR2 = $[\sum w(|F_o|^2 - |F_c|^2)^2/\sum wF_o^4]^{1/2}$, $w = [\sigma^2F_o^2 + (0.0256p)^2 + 2.1000p]^{-1}$, $p = [F_o^2 + 2F_c^2]/3$. **5**, 2534 ($I_o > 2\sigma I_o$), R1 = $\sum(||F_o| - |F_c||)/\sum|F_o|$, wR2 = $[\sum w(|F_o|^2 - |F_c|^2)^2/\sum wF_o^4]^{1/2}$, $w = [\sigma^2F_o^2 + (0.0180p)^2]^{-1}$, $p = [F_o^2 + 2F_c^2]/3$. **7**, 6629, R1 = $\sum(||F_o| - |F_c||)/\sum|F_o|$, wR2 = $[\sum w(|F_o|^2 - |F_c|^2)^2/\sum wF_o^4]^{1/2}$, $w = [\sigma^2F_o^2 + (0.0204p)^2]^{-1}$, $p = [F_o^2 + 2F_c^2]/3$. **9**, 5888 ($I_o > 2\sigma I_o$), R1 = $\sum(||F_o| - |F_c||)/\sum|F_o|$, wR2 = $[\sum w(|F_o|^2 - |F_c|^2)^2/\sum wF_o^4]^{1/2}$, $w = [\sigma^2F_o^2 + (0.0285p)^2]^{-1}$, $p = [F_o^2 + 2F_c^2]/3$.

Table 5. X-ray Crystallographic Data for Complex **12**·2CH_2Cl_2

crystal data	**12**·2CH_2Cl_2
empirical formula	$C_{44}H_{52}N_4O_{16}F_{12}S_4U{\cdot}2CH_2Cl_2$
crystal habit, color	block, brown
crystal size (mm)	0.12 × 0.08 × 0.06
crystal system	monoclinic
space group	$P2_1/n$
volume (Å^3)	3248(1)
a (Å)	13.224(2)
b (Å)	16.179(3)
c (Å)	15.338(3)
α (°)	90
β (°)	98.158(3)
γ (°)	90
Z	2
formula weight (g/mol)	1895.0
density (calcd) (M g/m^3)	1.938
absorption coefficient (cm^{-1})	5.370
F_{000}	1824
radiation	Mo Kα, 0.71073 Å
data refinement	
final *R* indices[a]	$R_1 = 0.031$, w$R_2 = 0.054$
largest diff. peak and hole (e Å^{-3})	0.86 and −0.86

[a] Number of observed reflections: **12**·2CH_2Cl_2, 5505 ($I_o > 2\sigma I_o$), R1 = $\sum(||F_o| - |F_c||)/\sum|F_o|$, wR2 = $[\sum w(|F_o|^2 - |F_c|^2)^2/\sum wF_o^4]^{1/2}$, $w = [\sigma^2F_o^2 + (0.0268p)^2]^{-1}$, $p = [F_o^2 + 2F_c^2]/3$.

of relevant crystallographic data is found in Tables 3−5, and full details of all crystallographic analyses are provided in the CIF files.

DFT Calculations. The uranium center was described using the Stuttgart relativistic effective core potential,[54,55] which places 60 electrons in the core (complete shells 1s through 4f), and the remaining 32 electrons, corresponding to the 5, 6, and 7 shells, are treated explicitly. For the atoms in the ligands, the double-ζ basis set 6-31G* was employed. All of the calculations were carried out using the Gaussian 03 suite of codes for quantum chemistry.[56]

Acknowledgment. We are grateful to the Seaborg Institute at Los Alamos National Laboratory for support of this work. T.W.H. wishes to acknowledge NSERC (Canada) and the Seaborg Institute for postdoctoral fellowships. E.R.B. and P.J.H. were supported by the Division of Chemical Sciences, Office of Basic Energy Sciences, U.S. Department of Energy, under the Heavy Element Chemistry program at Los Alamos National Laboratory. We would also like to thank Phillip D. Palmer for help with the UV/vis measurements.

Supporting Information Available: Complete details of the X-ray crystallographic studies as CIF files, geometries of the various isomers of the model complex **1** and complex **2**, and a complete version of ref 56. This material is available free of charge via the Internet at http://pubs.acs.org.

JA0629155

(54) Cao, X.; Dolg, M.; Stoll, H. *J. Chem. Phys.* **2003**, *118*, 487−496.
(55) Küchle, W.; Dolg, M.; Stoll, H.; Preuss, H. J. *J. Chem. Phys.* **1994**, *100*, 7535−7542.
(56) Frisch, M. J.; et al. *Gaussian 03*, revision C.02; Gaussian, Inc.: Wallingford, CT, 2004.